Hapten Immunetherapy for Liver Cancer HBV^{+} 40 Years and Restores Normal HBV^{-}

Baofa Yu[1, 2, 3, 4, 5, *], Jian Zhang[2], Yan Han[2], Feng Gao[1], Peng Jing[1], Guoqin Zheng[1], Guangyong He[1], Yanping Liu[1]

[1]Department of Oncology, TaiMei Baofa Cancer Hospital, Dongping 271500, China
[2]Department of Oncology, Jinan Baofa Cancer Hospital, Jinan 250000, China
[3]Department of Oncology, Beijing Baofa Cancer Hospital, Beijing 100068, China
[4]Lab, Immuno Oncology Systems, Inc., San Diego CA 92122, USA
[5]Shandong Medical and Pharmaceutical University, Yantai 264003, China

Abstract: Chronic hepatitis B virus (HBV) infection has considered a major risk factor for the development and progression of hepatocellular carcinoma (HCC), long-term lack of effective treatment worldwide. Hapten enhanced intratumoral chemotherap may provide a revival effect of immune system to against cancer cell of HCC and HBV. Methods. Single-cell RNA sequencing (scRNA-seq) was used to analyze the changes at the molecular level of tumor reflection from the untreated tumor after HEIC treated a few multi-focal HCC tumors. Results. After treatment with major tumors, both BMEM and Naive B cells, significantly increased MHC II signaling pathway-related genes, while plasma cells upregulated MHC I-related genes. Fibroblast, γδT/NK cells and Neutrophils, while NKT cells, Plasma cells, Endothelial cells, and B cells and M2 Macrophage showed values of AUC less than 0.6 which indicated minor affection or possible minor contribution to the therapeutic effect. It was observed significantly reduced scores of HBV-infection pathways, the percentages of CSTA+DCs and Kupffer cells were reduced, showing accordance with the attenuated HBV caused inflammation. Patient of HCC HBV DNA titter drop to zero and got control of the multifocal masses of HCC who still live. It is first discovered hapten is modifiing neo HBsAg (HBsAg) while it is modifying the TAAs's epitope, which return to a *neo* HBsAg, *neu* TAAs and rejuvenate a revival effects of immune system against cancer and HBV, i.e., by activating efficacy of CD4 T-cell activation and CD8 T-cell responses, thus, prolonging the survival time of patients, and maintaining the quality of life. Conclusions. This study provides new biological knowledge of therapy, hapten based intratumoral chemoimmunotherapy is playing an important role to improve *neu* TAAs and *neo* HBsAg for a revival of immune effect to control cancer cell and HBV in HCC with HBV positive.

Keywords: Immunotherapy; SscRNA-seq; Liver Cacner with HBV; HBV Vaccine; HBsAg-based Immune Therapy

DOI: 10.57237/j.wjcm.2026.01.002

1 Introduction

The burden of hepatocellular carcinoma (HCC) has progressively declined in the United States and increasing in China, and the distribution of tumors in China and the United States is converging. [1] Multi-focal HCC tumors that develop from primary intrahepatic metastasis (IM) or multi-center progression (MO) are a major feature of hepatocellular carcinoma (HCC). [2] Chronic hepatitis B virus (HBV) infection has long been considered a major risk factor for the development and progression of hepatocellular carcinoma (HCC) through direct and indirect mechanisms,

*Corresponding author: Baofa Yu, bfyuchina@126.com

Received: 9 March 2026; Accepted: 15 April 2026; Published Online: 27 April 2026

with HBV causing more than half of all HCC cases worldwidely. The transformation of HBV infected liver into HCC is mainly the result of long-term interactions between HBV and host hepatocytes through multiple mechanisms, including HBV DNA integration, prolonged expression of viral HBV regulatory proteins and/or preS/S envelope proteins, and epigenetic dysregulation of tumor suppressor genes. [3] Surgery is the preferred treatment for early stage of HCC. Among HCC multifocal tumors, only a minority of HCC patients survive longer under the control of immune surveillance, while other HCC patients have a poorer prognosis due to various mechanisms that evade the immune system. [2] Local therapy and new treatment options remains a necessary for the treatment of primary multifocal HCC. [4] Immunotherapy has emerged as a new treatment opportunity for multifocal liver cancer like programmed death-1 (PD1) or programmed death-ligand 1 (PD-L1) blockers, it has also been successful in showing some promise. [5]. Hapten combined chemotherapy has been successfully injected into liver cancer tumors, prolonging survival and maintaining patients' quality of life. [6] It works by killing the tumor, releasing the tumor-associated antigens (TAAs) with hapten modifying at same time to turn TAAs to *neo* TAAS and producing an effective DC through antigen presentation, thereby generating an immune response in the whole body and untreated tumor area. These antigens are modified by haptens and act as immunomodulators to alter tumor epitopes of tumor antigens. This immune response may be reflected in distal tumors in the form of proximal distal effects in many kind of lung and liver cancer patients. [6-8] New treatments for HBV-positive multifocal liver cancer have not been reported.

Hapten enhanced intratumoral chemotherapy (HEIC), which uses small molecules as haptens with chemical drugs injected into tumor, it kill tumor cells and release tumor antigens. [9-11] These antigens are modified by hapten and turn into *neo* antigens, which are then presented by dendritic cells to initiate and activate the action of tumor vaccines and stimulate the immune system. HEIC has shown promise in generating tumor-specific T cell immune responses like cytokines such as IFN-γ, IL-4, which can be further enhanced when combined with other immunotherapies like PD1. [9, 12-14] HEIC induced significant *in vitro* effects of B cell immune system associated with increases of autologous antibodies of p53, P16, RalA, Survivin, Zeta, Cmyc, HCC1, NPM1, IMP1, [10, 13, 14] suggesting a strong immune response. HEIC mediates and enhances the crosstalk between tumors and immunity, resulting in increased anti-TAAS antibodies and immune cytokines that kill tumors. [11, 13, 14] HEIC was successful application to HCC treatment including huge size and multifocal tumors of HCC [15, 16].

Single-cell RNA sequencing (scRNA-SEQ) is a new technology, thousands of cells can be evaluated simultaneously and complex cellular regulation, communication, and interactions can be revealed before and after HEIC therapy. [17]

The current scRNA-SEQ on HCC mostly focus on the tumor microenvironment (TME), [18] lacking in comparison of *in vitro* effects related to liver cancer immune responses at the single-cell level of untreated tumors. There is no publication about comparison of hapten-enhanced local chem-immuotherapy before and after an primary HBV-positive HCC with multiple focal tumors and restore to abnormal HBV negative.

Hapten was employed in the immunotherapy of HPV-associated lession due to hapten treating HPV16-E7 protein and turn into vaccine of HPV. [19-21] We can expect that HEIC kill liver cancer cells and hapten modify the product of HBV like protein HBx and/or altered versions of the preS/S envelope proteins on cellular chromatin and specific gene loci and turn into HBV vaccine.

In this study, we applied scRNA-Seq to tumor tissues of multiple tumor primary sites before and after treatment of tumors, and analyzed untreated tumor samples to explore the relationship between the response of inducing immune to tumor therapy.

In addition, we comprehensively characterized the malignant epithelial cells and various immune cells, and heterogeneity of cell subtypes, changes in HBV expression at cellular and molecular levels of HBV and blood HBV titers. This study provides new biological knowledge on the T and B cell at sing cell level of untreated tumors before and after intratumoral injection of haptens plus chemotherapy agents in primary focal tumors.

2 Materials and Methods

2.1 Sample Collection

The liver cancer samples used in this study were collected from patient with multifocal tumors of HCC by pathological and PETCT confirmation and this experiment was approved by the Ethics Committee Board of Shandong Baofa Cancer Institute (TMBF 0010, 2015) for therapy and participation in the study prior to commencing. a small primary mall tumor biopsied from the primary major tumor was used as window for scRNA-SEQ analysis, this tumor was not treated at all, at time point of before and after primary major tumor treat for intratumoral injection of cytotoxic drugs plus hapten (Figure

1 Graphic abstract) in Taimei Baofa Cancer hospital. The patient with high abnormal HBV and Alpha-fetoproteins (AFP)-negative (AFP≤20 ng/mL) was detected by blood test and diagnosed as hepatocellular carcinoma at a general hospital in Beijing. Then the blood was taken again to detect circulating tumor cells (CTC). [23] His HBV titter is very high for 2.14×10^5 ng/ml. All experiments were conducted after approval by the Ethics Committee Board of Shandong Baofa Cancer Institute (ID: TMBF 0010, 2015), and the participating patient also signed informed consent forms.

2.2 Single Cell RNA-seq: Cell Preparation, Library Construction and Sequencing

After the fresh tumor samples and blood were obtained. First, the samples were washed with Hanks Balanced Salt Solution (HBSS). The single-cell suspensions were prepared using enzymolysis, followed by preparing single-cell RNA-seq libraries using SeekOne® Digital Droplet (SeekOne® DD) Single Cell 3' library preparation kit. The prepared libraries were cleanup with SPRI beads, quantified by quantitative PCR (KAPA Biosystems KK4824) and then sequenced on Illumina NovaSeq 6000 in NovaSeq in Novogene, Co. Ltd (Beijing, China).

2.3 Bioinformatic Analysis

The pipeline of processing the raw reads, cell filtering and annotation were manually performed referring to the references. [22, 23] In brief, the clean reads filtered by fastp software (version 0.23.2) [24] were used to generate transcript expression matrix with SeekSoul tools. Cell filtering and annotation were carried out using the package Seurat. [25]. The poor-quality cells were flagged when they met one of the following thresholds: 1) number of features (nFeature_RNA) < 400 or nFeature_RNA > 7,000; 2) the number of reads (nCount_RNA) < 500 or nCount_RNA > 80,000; and 3) total percentages of mitochondrial genes > 5% or ribosomal genes > 40%. DoubletFinder package were employed to identify singlet cells, [26] followed by cluster identification and annotation based on classical cell markers. Gene set enrichment analysis (GSEA) based on the differentially expressed genes (DEGs), and GSVA were employed for functional enrichments analysis. [27-29] A tool prioritizing the responsiveness of a population to experimental perturbations, was used with default parameters to calculate the perturbation prioritization of different cell types in response to treatment. The functional activities of T cells were estimated using GSAV and the gene sets of Naive (*IL7R, CCR7, SELL, FOXO1, KLF2, KLF3, LEF1, TCF7, ACTN1, FOXP1*), Activation effector function (*FAS, FASLG, CD44, CD69, CD38, KLRF1, FOXP1, KLRG1, FCGR3A, CX3CR1*), Exhaustion (*PDCD1, LAYN, HAVCR2, LAG3, CTLA4, TOX, VSIR, BTLA, ENTPD1, CD160*), TCR Signaling (*CALM1, CALM2, CALM3, CAST, GNLY, PRF1, CD3D, CD3E, CD3G, CSK*), Cytotoxicity (*GZMA, GZMB, GZMH, GZMK, GZMH, NKG7, PRF1, KLRF1, KLRK1, FCGR3A*), Cytokine receptor, (*CSF1, IL10RA, IL16, IL17RA, IL18RAP, IL21R, IL2RB, IL2RG, IL32, IL9R*), Chemokine receptor (*CCR4, CCR5, CCR7, CXCR3, CXCR4, CXCR5, CXCR6, CXCL13, CXCL8, CCL3*), Senescence (*NT5E, IZUMO1R, LAG3, CBLB, DOK1, DOK2, SERPINB1, SERPINB6, SERPINB9, ADAM10*), Anergy (*NFKB1, NFKB2, NFKBIA, NFKBIB, NFKBIZ, CHUK, IKBKB, IKBKG, RELA, RELB*), NFKB Signaling (*HIKESHI, UBA52, RPA2, RPA3, MAP2K1, MAP2K2, MAP2K3, MAP3K4, MAP3K5, MAP3K8*), Stress response (*MAP2K1, MAP2K2, MAP2K3, MAP3K4, MAP3K5, MAP3K8, MAPK1, MAPK1, MAPK11, MAPK13*), MAPK Signaling (*ITGA1, ITGA4, ITGAE, ITGAL, ITGAM, ITGB1, ITGB2, ITGB7, SELL, SELPLG*), Adhesion (*IFIT1, IFIT2, IFIT3, IFIT5, STAT1, STAT2, IRF1, IRF4, IRF7, IRF8*), IFN Response (*ATP1B3, ATP2A3, ATP2B1, ATP2B4, ATP5A1, ATP5B, ATP5C1, ATP5D, ATP5E, ATP5EP2*), Oxidative phosphorylation (*SLC2A3, SLC2A8, SLC2A8, PFKFB3, ALDOA, PGAM1, PGK1, PKM, LDHA, LDHB*), Glycolysis, (*ACAA1, ACADM, ACADVL, ACSL5, ALDH16A1, ALDH9A1, ALDH9A1, BAK1, BAX, BID*), Fatty acid metabolism (*BCL2L11, BCL11B, BCL2L1, BIN1, BIN2, BIN1, BAG3, BAG4, BAK1, BAX*), Pro apoptosis (*BCL2L11, BCL11B, BCL2L1, BIN1, BIN2, BIN1, BAG3, BAG4, BAK1, BAX*), Anti apoptosis (*BCL2L1, BCL11B, BCL2L1, BIN1, BIN2, BIN1, BAG3, BAG4, BAK1, BAX*) [30, 31]. Monocle2 [32] and CytoTRACE [33] were employed to infer developmental trajectories of cells within same broad type. CellChat packages with default parameters was employed to predict cellular communications. [34] The built-in tests in the softwares were employed acquiescently to calculate adjusted *p* values at a significance threshold of $adj.p < 0.05$.

3 Results

3.1 Clinical Benefit Characteristics

The blood sample was collected for circulation tumor

cells count for hepatocellular carcinoma, CTC was detected, and it showed CTC numbers decreased from 48/3ml (before treatment) to 3/3ml one week later, and CTC further decreased to 1/3ml two weeks later (after treatment). It indicates that the tumor was controlled, and fewer live tumor cells were released into blood circulation after treatment. CT and color ultrasonic imaging showed the tumor was stable and under control with the tumor. PETCT showed that there is no activity of F18-FDG in the scope of the tumor area at one years later. The abnormal HBV DNA level was observed as greatly decreased 2.14×10^5 ng/ml to 8×10^2 ng/ml 30 days after the first treatment and less 40 iu/ml at 180 days after first treatment, at 1 year time of treatment, he is living normal as normal person.

3.2 Landscape of Sing-cell Atlas of HBV-infected Liver Before and After Treatment

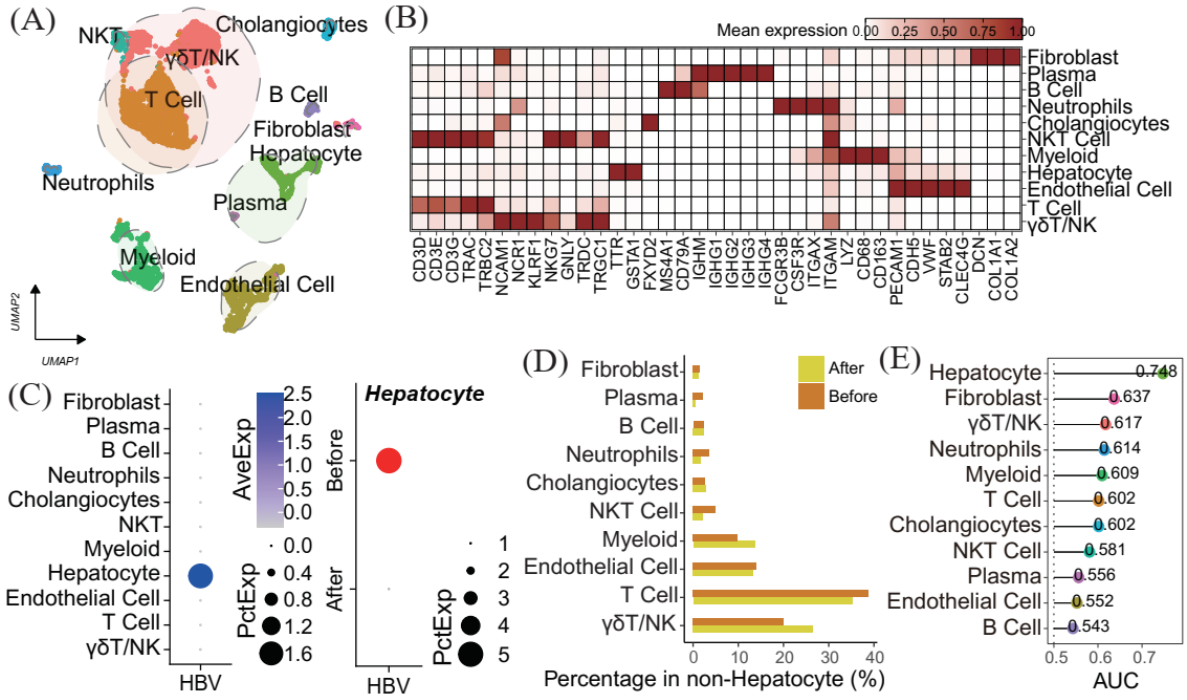

Figure 1 Landscape of sing-cell atlas. UMAP visualization illustrating the cell types (A), and heatmap illustrating marker genes of different cell types (B). (C) Dot plot comparing the levels of HBV reads in different cell types, and the HBV levels in Hepatocyte between the Before group and the After group. (D) Bar plot comparing the percentages of non-Hepatocytes between the Before group and the After group. (E) AUC values calculated by Augur for different celltypes

As shown in Figure 1A, a total of eleven broad cell types were assigned, including Fibroblast cells, Plasma cells, B cells, Neutrophils, Cholangiocytes, NKT cells, Myeloid, Hepatocytes, Endothelial cells, T cells, and γδT/NK cells. Their cell markers were shown in Figure 1B. HBV reads were only detected in Hepatocytes. Moreover, the percentage of HBV-infected Hepatocytes were reduced from 5.05% in Before group to 0.1% in after group (Figure 1C), further demonstrated the effective therapeutic effect in this study. The percentages of different broad cell types in the two groups were shown in Figure 1D and Table 1. In comparison to the before group, we observed possible reduction in the infiltration of Plasma cells, Neutrophils and NKT cells, as well as possibly increased Myeloid and γδT/NK, in after group. The machine learning algorithm augur were employed to estimate the perturbation prioritization of different cell types in response to treatment (Figure 1E). The Hepatocytes was the most affected cells with AUC scores of 0.748 far ahead others', which was in accordance with the effective therapeutic effect in this study. The followed three affected cell types were Fibroblast (AUC = 0.637), γδT/NK cells (AUC = 0.617) and Neutrophils (AUC = 0.614), while NKT cells, Plasma cells, Endothelial cells, and B cells showed values of AUC less than 0.6 which indicated minor affection or possible minor contribution to the therapeutic effect.

3.3 GSVA Scores of KEGG Pathways in Hepatocytes and Neutrophils

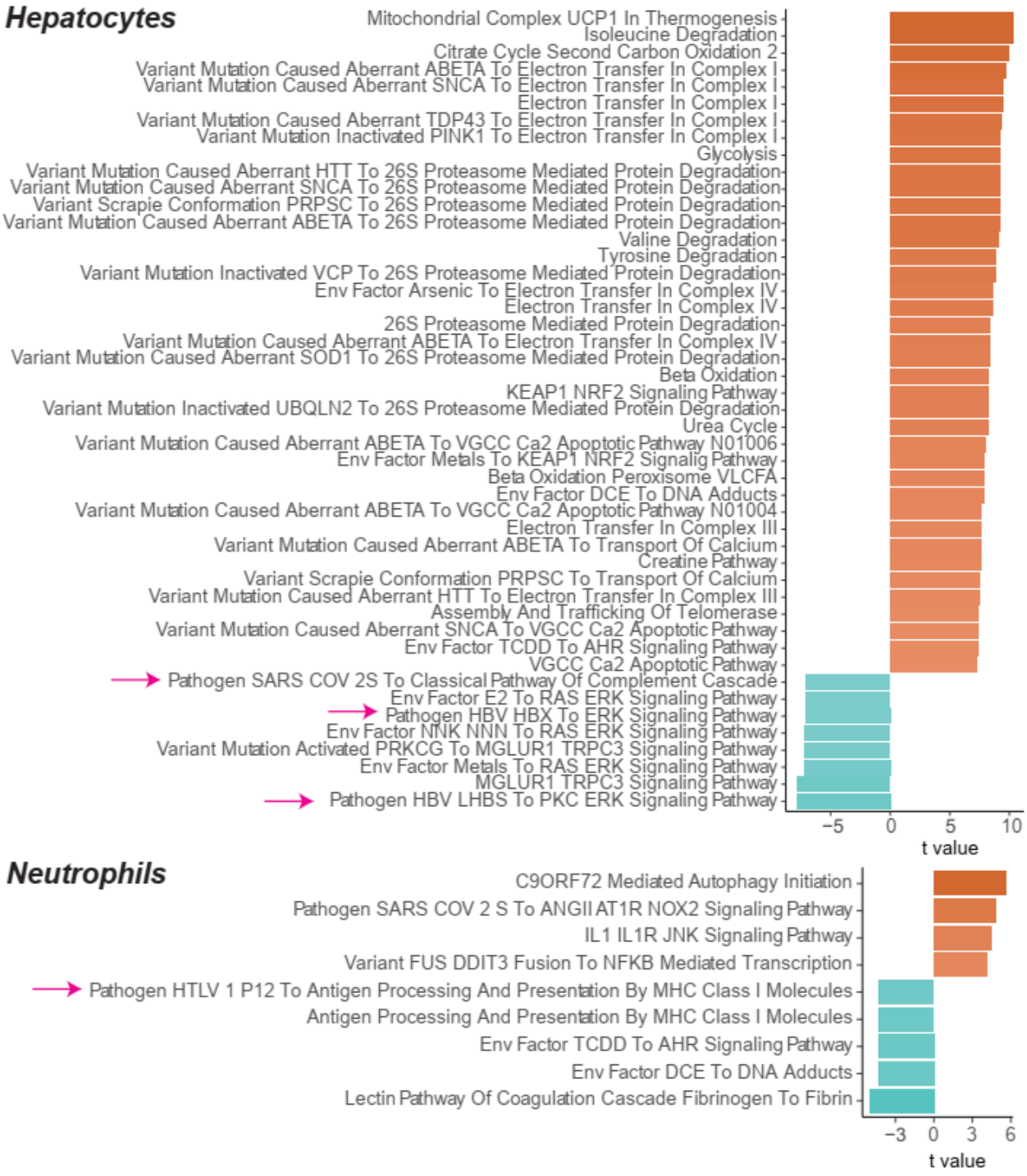

Figure 2 Comparison of the GSVA scores of KEGG pathways between the After group *vs* the Before group

To further verify the therapeutic effect, GSVA against KEGG was then performed on the Hepatocytes and Neutrophils in before and after groups. As shown in Figure 2, we observed significantly reduced scores of HBV-infection pathways (e.g., Pathogen HBV HBX To ERK Signaling Pathway, Pathogen HBV LHBS To PKC ERK Signaling Pathway) in Hepatocytes in after group compared to the before group. The pathway "Pathogen SARS COV 2S To Classical Pathway of Complement Cascade" was reduced in after group when compared to the before group, suggesting same conclusion as well.

In Neutrophils, we observed reduced pathway "Pathogen HTLV 1 P12 To Antigen Processing and Presentation By MHC Class I Molecules" in after group when compared to the before group. C9ORF72 mediated autophagy has been demonstrated to play important roles in inflammation suppression [35, 36], further demonstrating that the HBV-caused inflammation has been attenuated after treatment.

3.4 The Variations in Myeloid and Fibroblast

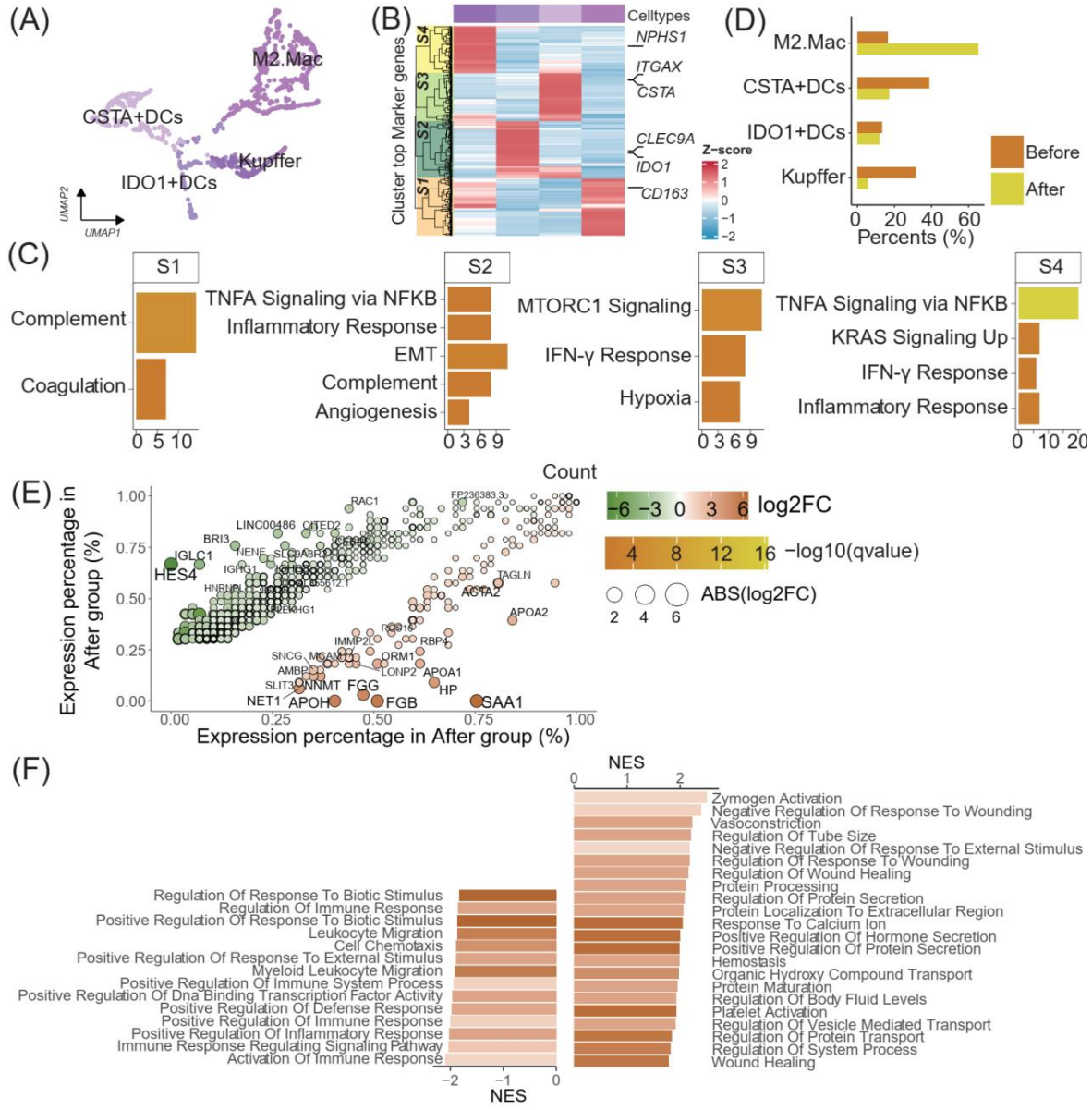

Figure 3 The Myeloid and Fibroblasts in Before and After groups. (A) UMAP visualization illustrating the subpopulations of Myeloid, and (B) heatmap illustrating the top 100 markers in different in different feature sets (S1 ~ S4) revealed by NMF. (C) The KEGG pathways enriched with the NMF feature sets. (D) The percentages of subpopulations in Myeloid. The DEGs of Fibroblasts between Before group and After group (E), and the NES values of KEGG pathways calculated with the DEGs (F)

The NMF was employed to extract the signatures and cluster the subpopulations of Myeloid, which indicated that k=5 (Figure 3A). The Myeloid was clustered into M2 Macrophage, CSTA$^+$DCs, IDO1$^+$DCs, and Kupffer cells (Figure 3B). The four feature sets (S1 ~ S4) uncovered by NMF were then enriched against Hallmarker pathways. As shown in Figure 3C, the S1 highly expressed in M2 Macrophage were enriched into Complement and Coagulation, the S2 highly

expressed in IDO1^{+}DCs were enriched into TNFA Signaling via NFKB, and Inflammatory Response, the S3 highly expressed in CSTA^{+}DCs were enriched into MTORC1 Signaling, and IFN-γ Response, the S4 highly expressed in Kupffer were enriched into TNFA Signaling via NFKB, and Inflammatory related pathways (Figure 3C). These observations indicated that CSTA^{+}DCs, IDO1^{+}DCs, and Kupffer cells were pro-inflammatory, while M2 Macrophage was found to be potential complement producer. After treatment, the percentages of CSTA^{+}DCs and Kupffer cells were reduced, showing accordance with the attenuated HBV-caused inflammation (Figure 3D). The DEGs of Fibroblasts between After group and Before group were shown in Figure 3E. The DEGs revealed upregulated pathways related to normal liver functions (NES > 1, *q value* < 0.05), while the pathways related to the immune response and inflammation were downregulated (NES < -1, *q value* < 0.05).

3.5 T Cells' Atlas Highlighted Effective Memory CD8^{+}T Cells (CD8^{+}Tem)

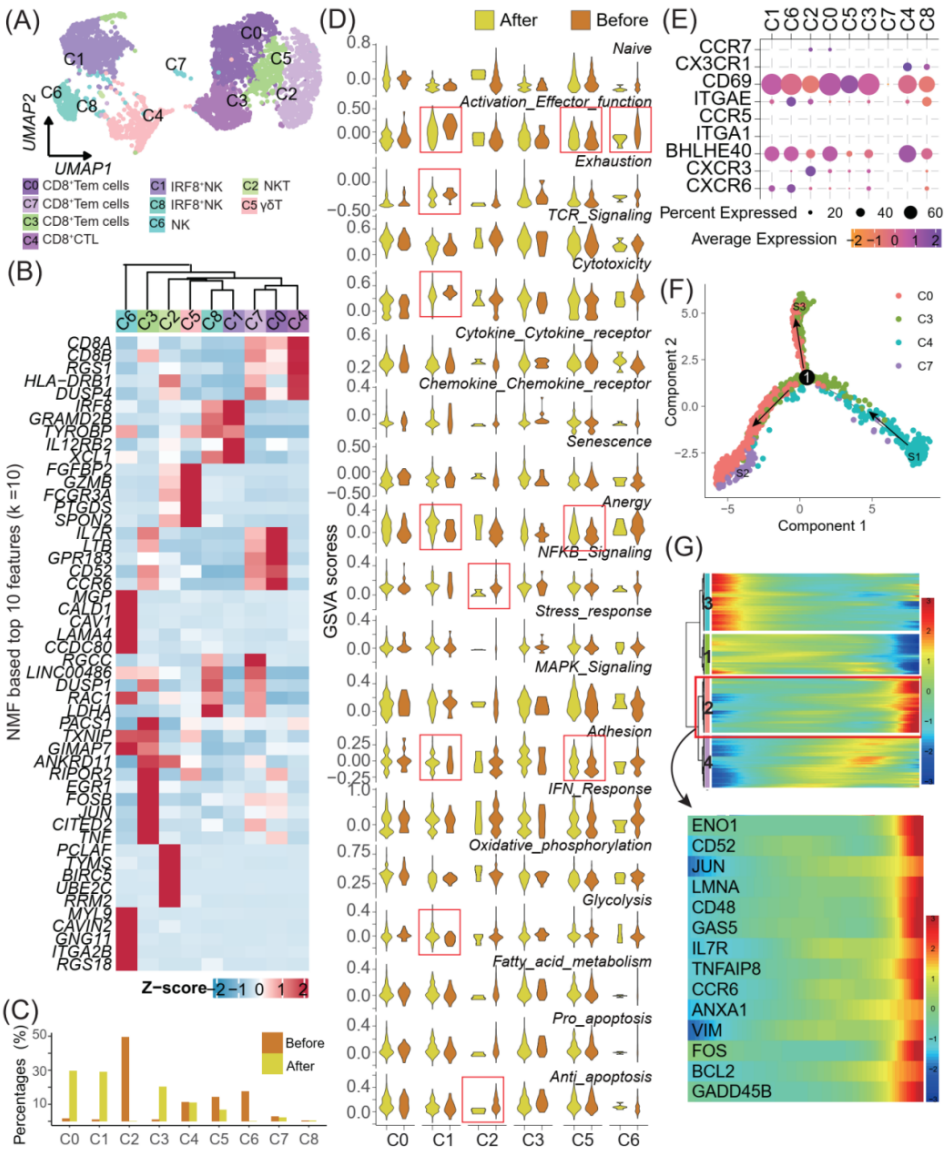

Figure 4 The T/NK/NKT cells in Before and After groups. (A) UMAP visualization illustrating the subpopulations of T/NK/NKT cells, and (B) heatmap illustrating the top 10 markers in different in different feature sets revealed by NMF. (C) The percentages of subpopulations in T/NK/NKT cells in the two groups. (D) The GSVA scores estimating the activities of the subpopulations in the T/NK/NKT cells. (E) Dot plot illustrating the expression levels of Trm related genes in the subpopulations in the T/NK/NKT cells. (F) Monolce2 pseudo-trajectory of C0, C3, C4 and C7 in CD8^{+}T cells. (G) Heatmap illustrating the genes expression along with pseudo-time

By employing NMF, the T/NK/NKT populations were clustered into nine clusters assigned into CD8$^+$Tem, CD8$^+$CTL, IRF8$^+$NK, NK, NKT and γδT cells (Figure 4A and B). The percentages of clusters C0 and C3 in CD8$^+$Tem, and the C1 in IRF8$^+$NK were increased in after group compared to the before group, while the percentages of C2 in NKT and C6 in NK, C5 in γδT were impaired (Figure 4C). To thoroughly estimate the activities of these subpopulations, single cell GSVA against 19 signature sets were carried out (Figure A1). The increased C0 and C3 did not perform highest cytotoxicity but perform lower exhaustion. In addition, no significant difference in the 19 signature sets was observed between after group and before group in either C0 nor C3 (Figure 4D). The clusters C0, C1 and C3 were found to express high levels of tissue resident markers CD69, BHLHE40 and CXCR6 (Figure 4E). Therefore, the augmented differentiation to C0 and C1 were supposed to play crucial roles in control HBV. We then performed pseudo-trajectory analysis on the C0, C3, C4 and C7 (Figure 4F). It was found increasing expression of genes related to effector and memory of T cells along the pseudo-trajectory (Figure 4G).

Table 1 Cell subtypes and cell numbers of each sample by tissue dissociation

CellType	liverCa_B	liverCa_A
B_cell	46 (1.77%)	106 (1.98%)
Endothelial_cells	204 (7.84%)	396 (7.38%)
Hepatocytes	442 (16.98%)	997 (18.58%)
Macrophage	152 (5.84%)	650 (12.11%)
Monocyte	93 (3.57%)	129 (2.4%)
Neutrophils	156 (5.99%)	114 (2.12%)
NK_cell	660 (25.36%)	1390 (25.9%)
Smooth_muscle_cells	41 (1.58%)	58 (1.08%)
T_cells	809 (31.08%)	1527 (28.45%)
Total	2603 (100%)	5367 (100%)

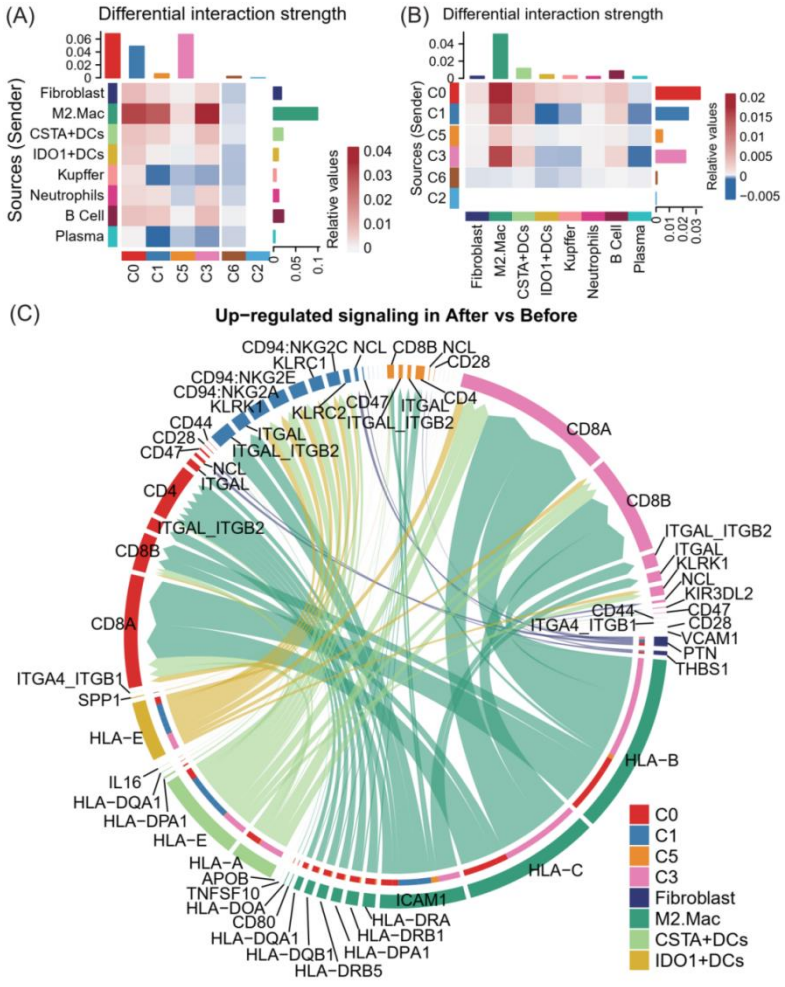

Figure 5 The cellular communications predicted using CellChat. Heatmap showing the differential interaction strength from non-T/NK/NKT immune cells to T/NK/NKT cells (A) and from T/NK/NKT cells to non-T/NK/NKT immune cells (B). (C) Chord diagram presenting the upregulated cellular communications

We then focused on the cellular communications between non-T/NK/NKT immune cells and C0, C2, C1, C3, C5, C6. No significant communication was found referring to C2, while we found high levels of cellular communications referring to C0 and C3, especially the upregulated communications between Macrophage/CSTA^{+}DCs/IDO1^{+}DCs and C0/C3 (Figure 5A and B). In details, the communications between Macrophage/CSTA^{+}DCs/IDO1^{+}DCs and C0/C3 were mainly enriched in pathways of activating T cells, such as those receptors were CD8A, CD8B, CD28, CD4 (Figure 5C, A2).

4 Discussion

Few drugs and treatment strategies are available for progressed or later stages of liver cancer with multifocal tumors. Local and novel treatments, i.e. immunotherapies, are necessary to treat cancer at later stages. [14, 16] Tumor-local treatment kills tumor-induced immune reactions, and this therapy has also achieved some success and shows a certain future for cancer treatment. [16] Hapten combined with chemotherapeutic drugs has been successfully injected into the tumor to treat liver cancer, hapten is an immune modulator and modifies the TAAs's epitope, meanwhile hepatitis B surface antigen (HBsAg) is also modified, which became a *neu* TAAs, *neo* HBsAg, and rejuvenate a revival effects of immune system against cancer and HBV, i.e., prolonging the survival time of patients, and maintaining the quality of life. [17] here, *neo* HBsAg like HBV Vaccines, however, the key determinants required to overcome HBV-specific immune tolerance, combination adjuvants and unravel factors that are essential for the antiviral efficacy of TherVacB, CD4 T-cell activation during the priming phase of TherVacB as a key determinant of HBV-specific antibody and CD8 T-cell responses. [43-45]

Clinical benefits of this study were obvious from the patient's daily quality of life and the patient's feeling s about everything better than before treatment over 12 months. It was found that after HEIC treatment, biopsies were taken again from multiple small masses in the scope of the big tumor area, and the tumor cells with the lowest activity were less than 3%, also loss quality of activity to do any single-cell sequencing. It showed CTC numbers decreased from 5/3ml at the time before treatment to 0/3ml one week later (after treatment). It indicated this therapy benefits the patient's quality of life without any side effects that happened until the last visit of clinical 11 months from the first treatment. It showed affected cell types were Fibroblast (AUC = 0.637), γδT/NK cells (AUC = 0.617) and Neutrophils (AUC = 0.614), while NKT cells, Plasma cells, Endothelial cells, and B cells and M2 Macrophage showed values of AUC less than 0.6 which indicated minor affection or possible minor contribution to the therapeutic effect. The percentages of clusters C0 and C3 in CD8+Tem, and the C1 in IRF8+NK were increased in after group compared to the before group, while the percentages of C2 in NKT and C6 in NK, C5 in γδT were impaired.

The abnormal HBV DNA level was observed for less 40 iu/ml at 180 days after first treatment, it indicated that HEIC has additional function for control HBV by induce HBV immune response. We observed significantly reduced scores of HBV-infection pathways, C9ORF72 mediated autophagy has been demonstrated to play important roles in inflammation suppression [35, 36], further demonstrating that the HBV-caused inflammation has been attenuated after treatment. After treatment, the percentages of CSTA+DCs and Kupffer cells were reduced, showing accordance with the attenuated HBV-caused inflammation (Figure 3D). The percentages of M2 Macrophage were increased, suggesting probably increasing complement levels to play important roles in control HBV-infection. [37] Moreover, HBV has been found to inhibit the expression of complement in vitro and in vivo, [38] the increased M2 Macrophage with high capability of producing complement might be benefit function recovery of liver.

It is acknowledgedly recognized that exhausted CTL greatly contributed to chronic HBV infection in liver, because of their dull immune response to HBV. [39]. The recovered CD8+Tem (C0 and C3) with lower exhaustion might promise the HBV seroconversion (Table 1 and Figure 1). The increased C1 and impaired C6 did not show significant difference across the 19 signature sets. However, the increased C1 of IRF8+NK were supposed to play important roles in HBV seroconversion, since IRF8 has been reported to orchestrates the adaptive NK cell response to severe viral infection in humans. [40] HBV-specific tissue resident memory T cells (Trm) play key roles in suppressing HBV (Figure 4E). [41]Therefore, the augmented differentiation to C0 and C1 were supposed to play crucial roles in control HBV. We then performed pseudo-trajectory analysis on the C0, C3, C4 and C7 (Figure 4F). We found increasing expression of genes related to effector and memory of T cells along the pseudo-trajectory (Figure 4G).

[42] The communications between Macrophage/CSTA+DCs/ IDO1+DCs and C0/C3 were mainly enriched in pathways of activating T cells, such as those receptors of CD8A, CD8B, CD28, CD4.

In short, the abscopal effect is a complex immunity reaction and it can be induced by hapten with chemotherapy drugs intratumoral injection, that is not only involves B cell activity but also involves T cell activity with multiple genes participating at the molecular level, and it can be used to treat multilocal tumor in live of HCC; which plays an important role to improve *neu* TAAs and *neo* HBsAg and induce a revival of immune effect to control cancer cell and HBV virus, haptem modified *neo* HBsAg may overcome the HBV-specific immune tolerance and short efficacy of monotherapy with HBsAg-based immune therapy and less control of HBV replication and/or liver damages, which approved by activating immune cell like CD8 and CD4. This discovery has matched our clinical finding of HBV DNA titter drop to zero and many cases of HCC with hepatitis B virus (HBV) & cirrhosis had been improvement for their cirrhosis condition in past time. Finally, further detailed studies with more multifocal tumor of HCC patients thorough HEIC treatment are required to develop a comprehensive understanding of the full mechanism of therapeutic potential for HCC with and without chronic HBV and Chronic hepatitis B cirrhosis and sclerosing nodules.

Appendix

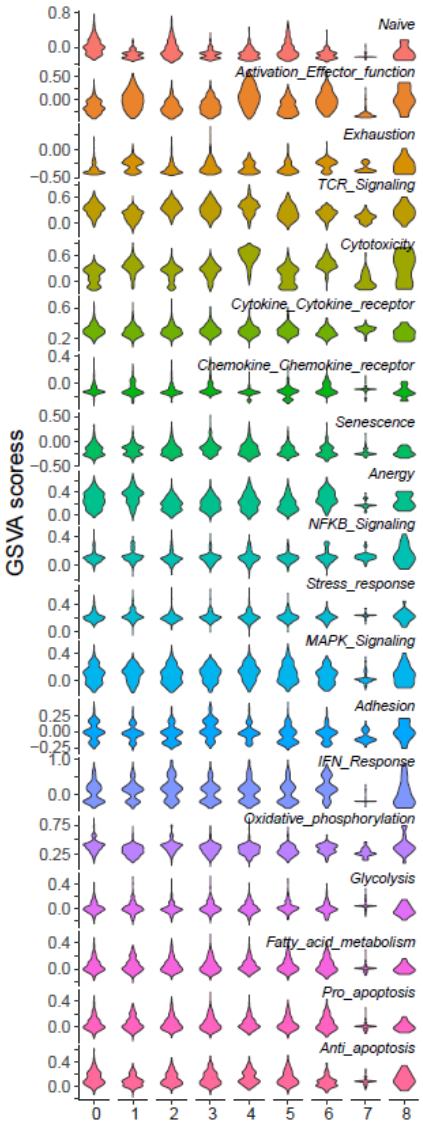

Figure A1 The GSVA scores estimating the activities of the all subpopulations in the T/NK/NKT ells

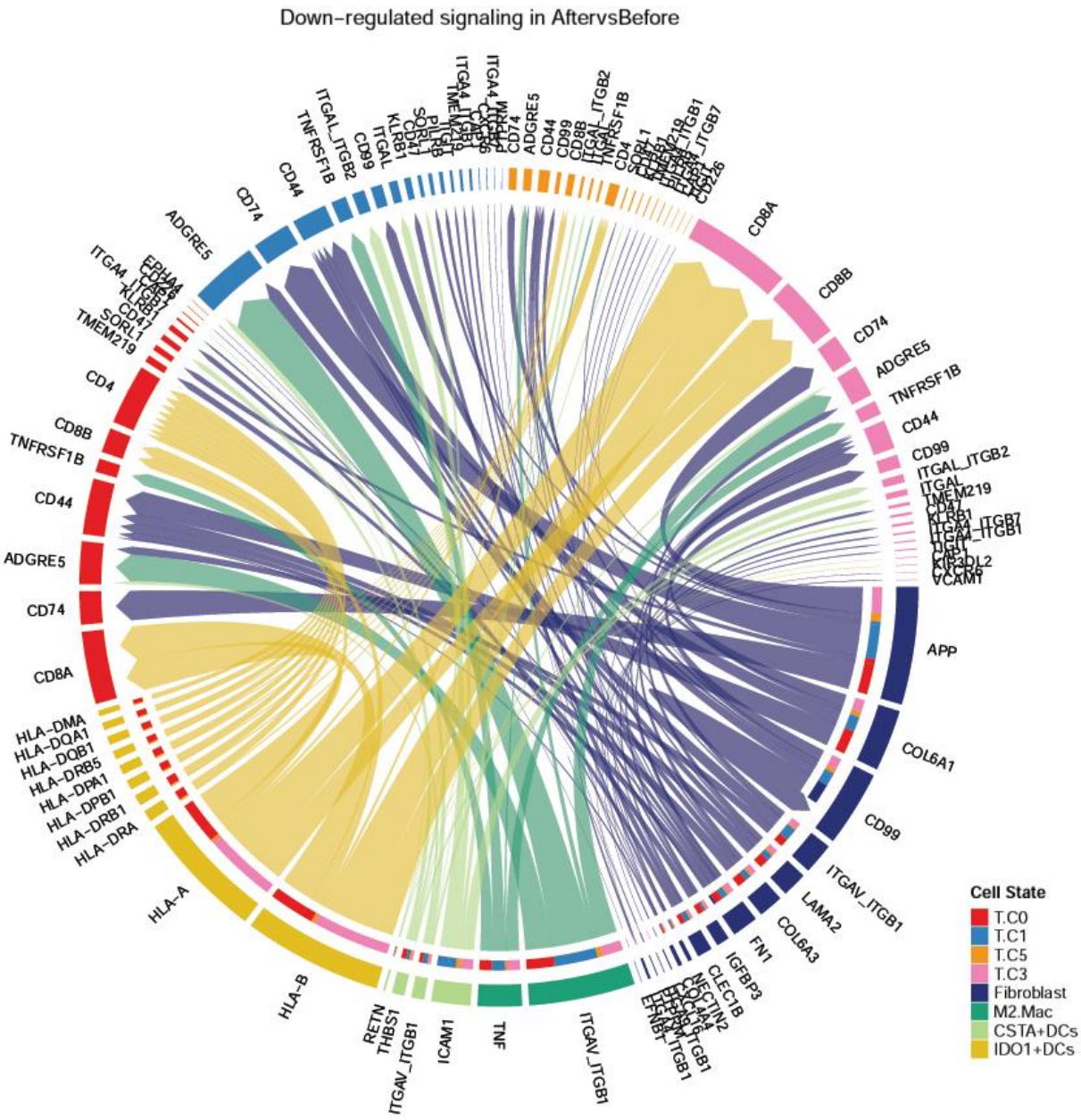

Figure A2 Chord diagram presenting the downregulated cellular communications

References

[1] Xia C, Dong X, Li H, Cao M, Sun D, He S, et al. Cancer statistics in China and United States, 2022: profiles, trends, and determinants. Chinese medical journal. 2022; 135(05): 584-90. https://doi.org/10.1097/CM9.0000000000002108

[2] Liang-Qing Dong 1, Li-Hua Peng 2, Li-Jie Ma, et al. Heterogeneous immunogenomic features and distinct escape mechanisms in multifocal hepatocellular carcinoma. J Hepatol. 2020 May; 72(5): 896-908. https://doi.org/10.1016/j.jhep.2019.12.014

[3] L Jia, Y Gao, Y He, et al. HBV induced hepatocellular carcinoma and related potential immunotherapy. Pharmacol Res. 2020 Sep: 159: 104992. https://doi.org/10.1016/j.phrs.2020.104992

[4] Liu C-Y, Chen K-F, Chen P-J. Treatment of liver cancer. Cold Spring Harbor perspectives in medicine. 2015; 5(9): a021535. https://doi.org/10.1101/cshperspect.a021535

[5] Xu F, Jin T, Zhu Y, Dai C. Immune checkpoint therapy in liver cancer. Journal of Experimental & Clinical Cancer Research. 2018; 37(1): 1-12. https://doi.org/10.1186/s13046-018-0777-4

[6] Yu B, Lu Y, Gao F, Jing P, Wei H, Zhang P, et al. Hapten-enhanced therapeutic effect in advanced stages of lung cancer by ultra-minimum incision personalized intratumoral chemoimmunotherapy therapy. Lung Cancer: Targets and Therapy. 2015: 1-11. https://doi.org/10.2147/LCTT.S70679.eCollection 2015

[7] Gao F, Jing P, Liu J, Lu Y, Zhang P, Han W, et al. Hapten-enhanced overall survival time in advanced hepatocellular carcinoma by ultro-minimum incision personalized intratumoral chemoimmunotherapy. Journal of Hepatocellular Carcinoma. 2015: 57-68. https://doi.org/10.2147/JHC.S80756.eCollection 2015

[8] The Professional Committee of Integrated Diagnosis and Treatment of the Chinese Anti-Cancer Association, the Research Center of the National Association of Radiological and Therapeutic Clinical Medicine and the National Interventional Medicine Innovation Alliance. Clinical Practice Guidelines for Interventional Therapy for Advanced Pancreatic Cancer (Trial) (7th edition) Journal of Clinical Radiology 43 (10), 2024.

[9] Sakamoto, E., et al. Chemical- and Drug-Induced Allergic, Inflammatory, and Autoimmune Diseases Via Haptenation. Biology (Basel) 12(2023).

[10] Yu, B., et al. Awaken Immune Cells by Hapten Enhanced Intratumoral Chemotherapy with Penicillin Prolong Pancreatic Cancer Survival. J Cancer 14, 1282-1292 (2023). https://doi.org/10.7150/jca.82985.eCollection 2023

[11] Lu, Y. & Low, P. S. Folate targeting of haptens to cancer cell surfaces mediates immunotherapy of syngeneic murine tumors. Cancer Immunol Immunother 51, 153-162 (2002). https://doi.org/10.1007/s00262-002-0266-6

[12] Erkes, D. A. & Selvan, S. R. Hapten-induced contact hypersensitivity, autoimmune reactions, and tumor regression: plausibility of mediating antitumor immunity. J Immunol Res 2014, 175265 (2014). https://doi.org/10.1155/2014/175265

[13] Schrand, B., et al. Hapten-mediated recruitment of polyclonal antibodies to tumors engenders antitumor immunity. Nature Communications 9, 3348 (2018). https://doi.org/10.1038/s41467-018-05566-x

[14] Yu, B., et al. Successful targeting in situ of an oncogenic nuclear antigen by hapten induced tumor associated autoantibodies (iTAA). Sci Rep 13, 9902 (2023). https://doi.org/10.1038/s41598-023-36757-2

[15] Yu, B., et al: Hapten enhanced overall survival time in advanced hepatocellular carcinoma by ultro-minimum incision personalized intratumoral chemoimmunotherapy. Journal of Hepatocellular carcinoma, 2015: 2 57-78. https://doi.org/10.2147/JHC.S80756.eCollection 2015

[16] Yu, B., et al. Cancer new treatment series: Comparison immune changes of HCC by scRNA-Seq following HELC treatment one case study. Trends in Immunotherapy 2024, 8(2), 8937. https://doi.org/10.24294/ti.v8.i2.8937

[17] Ziegenhain C, Vieth B, Parekh S, Reinius B, Guillaumet-Adkins A, Smets M, et al. Comparative analysis of single-cell RNA sequencing methods. Molecular cell. 2017; 65(4): 631-43. e4. https://doi.org/10.1016/j.molcel.2017.01.023

[18] Ma L, Hernandez MO, Zhao Y, Mehta M, Tran B, Kelly M, et al. Tumor cell biodiversity drives microenvironmental reprogramming in liver cancer. Cancer cell. 2019; 36(4): 418-30. e6. https://doi.org/10.1016/j.ccell.2019.08.007

[19] Giannini A, et al. Outcomes of high-grade cervical dysplasia with positive margins and HPV persistence after cervical conization. Vaccines (Basel). (2023) 11(3): 698. https://doi.org/10.3390/vaccines11030698

[20] Tran LS, et al. Interleukin-17A promotes arginase-1 production and 2,4-dinitrochlorobenzene-induced acute hyperinflammation in human papillomavirus E7 oncoprotein-expressing skin. J Innate Immun (2015) 7(4): 392–404. https://doi.org/10.1159/000374115

[21] Liu X, et al. Chemical immune conization of precancerous cervical lesions awakens immune cells and restores normal HPV negative and abnormal proliferation. Frontiers in Immunology. 2024 (03) 1. https://doi.org/10.3389/fimmu.2023.1259723

[22] Wei, X., et al., Elevated enteric putrescine suppresses differentiation of intestinal germinal center B cells. Int Immunopharmacol, 2024. 128: p. 111544. https://doi.org/10.1016/j.intimp.2024.111544

[23] Shi, S., et al., CXCR6 defines therapeutic subtypes of CD4+ cytotoxic T cell lineage for adoptive cell transfer therapy in pediatric B cell acute lymphoblastic leukemia. International Immunopharmacology, 2024. 132. https://doi.org/10.1016/j.intimp.2024.111972

[24] Chen, S., et al., fastp: an ultra-fast all-in-one FASTQ preprocessor. Bioinformatics, 2018. 34(17): p. i884-i890. https://doi.org/10.1093/bioinformatics/bty560

[25] Hao, Y., et al., Integrated analysis of multimodal single-cell data. Cell, 2021. 184(13): p. 3573-3587.e29. https://doi.org/10.1016/j.cell.2021.04.048

[26] McGinnis, C. S., L. M. Murrow, and Z. J. Gartner, DoubletFinder: Doublet Detection in Single-Cell RNA Sequencing Data Using Artificial Nearest Neighbors. Cell Syst, 2019. 8(4): p. 329-337.e4. https://doi.org/10.1016/j.cels.2019.03.003

[27] Subramanian, A., et al., Gene set enrichment analysis: a knowledge-based approach for interpreting genome-wide expression profiles. Proc Natl Acad Sci U S A, 2005. 102(43): p. 15545-50. https://doi.org/10.1073/pnas.0506580102

[28] Wu, T., et al., clusterProfiler 4.0: A universal enrichment tool for interpreting omics data. The Innovation, 2021. 2(3): p. 100141. https://doi.org/10.1016/j.xinn.2021.100141

[29] Skinnider, M. A., et al., Cell type prioritization in single-cell data. Nat Biotechnol, 2021. 39(1): p. 30-34. https://doi.org/10.1038/s41587-020-0605-1

[30] Chu, Y., et al., Pan-cancer T cell atlas links a cellular stress response state to immunotherapy resistance. Nat Med, 2023. 29(6): p. 1550-1562. https://doi.org/10.1038/s41591-023-02371-y

[31] Tang, F., et al., A pan-cancer single-cell panorama of human natural killer cells. Cell, 2023. 186(19): p. 4235-4251.e20. https://doi.org/10.1016/j.cell.2023.07.034

[32] Cao, J., et al., The single-cell transcriptional landscape of mammalian organogenesis. Nature, 2019. 566(7745): p. 496-502. https://doi.org/10.1038/s41586-019-0969-x

[33] Gulati, G. S., et al., Single-cell transcriptional diversity is a hallmark of developmental potential. Science, 2020. 367(6476): p. 405-411. https://doi.org/10.1126/science.aax0249

[34] Zhang, Y., et al., CellCall: integrating paired ligand–receptor and transcription factor activities for cell–cell communication. Nucleic Acids Research, 2021. 49(15): p. 8520-8534. https://doi.org/10.1093/nar/gkab638

[35] Burberry, A., et al., C9orf72 suppresses systemic and neural inflammation induced by gut bacteria. Nature, 2020. 582(7810): p. 89-94. https://doi.org/10.1038/s41586-020-2288-7

[36] Cicardi, M. E. and D. Trotti, C9orf72 role in myeloid cells: new perspectives in the investigation of the neuro-immune crosstalk in amyotrophic lateral sclerosis and frontotemporal dementia. Ann Transl Med, 2024. 12(6): p. 120. https://doi.org/10.21037/atm-24-86

[37] Li, Q., et al., Lower level of complement component C3 and C3a in the plasma means poor outcome in the patients with hepatitis B virus related acute-on-chronic liver failure. BMC Gastroenterol, 2020. 20(1): p. 106. https://doi.org/10.1186/s12876-020-01258-3

[38] Zhu, C., et al., Hepatitis B virus inhibits the expression of complement C3 and C4, in vitro and in vivo. Oncol Lett, 2018. 15(5): p. 7459-7463. https://doi.org/10.3892/ol.2018.8223

[39] Ye, B., et al., T-cell exhaustion in chronic hepatitis B infection: current knowledge and clinical significance. Cell Death & Disease, 2015. 6(3): p. e1694-e1694. https://doi.org/10.1038/cddis.2015.42

[40] Adams, N. M., et al., Transcription Factor IRF8 Orchestrates the Adaptive Natural Killer Cell Response. Immunity, 2018. 48(6): p. 1172-1182.e6. https://doi.org/10.1016/j.immuni.2018.04.018

[41] HBV-Specific T(rm) Cells Correlate with Relapse-Free Survival in HCC. Cancer Discov. 2021 Sep; 11(9): OF6. https://doi.org/10.1158/2159-8290.CD-RW2021-103

[42] He, X., Tang R., Lou J., et al. Pseudo-trajectory inference for identifying essential regulations and molecules in cell fate decisions. J Biol Phys. 2024 Nov 14; 51(1): 2. https://doi.org/10.1007/s10867-024-09665-3

[43] Mahmood F., Xu R., Awan M U N., et al. HBV Vaccines: Advances and Development. Vaccines (Basel). 2023 Dec 18; 11(12): 1862. https://doi.org/10.3390/vaccines11121862

[44] Su J, Brunner L., Edanur Ates Oz E. A., et al. Activation of CD4 T cells during prime immunization determines the success of a therapeutic hepatitis B vaccine in HBV-carrier mouse models. J Hepatol. 2023 Apr; 78(4): 717-730. https://doi.org/10.1016/j.jhep.2022.12.013

[45] Akbar S. M. F., Al-Mahtab M., Uddin M. H., et al. HBsAg, HBcAg, and combined HBsAg/HBcAg-based therapeutic vaccines in treating chronic hepatitis B virus infection. Hepatobiliary Pancreat Dis Int. 2013 Aug; 12(4): 363-9. https://doi.org/10.1016/s1499-3872(13)60057-0